The energies used in these calculations are taken from the compilation of Rosenstock and co-workers[18] and the compilation given by McIver and co-workers.[21] The appreciably higher endothermicity in reaction 21 compared with that in (19) would result in a lower (and perhaps zero) rate of exchange of OD^- with CH_4 compared with that for exchange with H_2. Similar considerations apply to the absence of exchange between OD^- and $i\text{-}C_4H_{10}$.

(21) John E. Bartmess, Judith A. Scott, and Robert T. McIver, Jr., *J. Am. Chem. Soc.*, **101**, 6046 (1979).

Acknowledgments. This work was supported by grants from the National Science Foundation and the National Institutes of Health, and the donors of the Petroleum Research Fund, administered by the American Chemical Society. We thank Gladys Roberts for help in preparing this manuscript.

Photoelectrochemical Behavior of n-GaAs Electrodes in Ambient-Temperature Molten-Salt Electrolytes

P. Singh, K. Rajeshwar,* J. DuBow, and R. Job*

Contribution from the Department of Electrical Engineering and Department of Chemistry, Colorado State University, Fort Collins, Colorado 80523. *Received July 11, 1979*

Abstract: Photoelectrochemical (PEC) characterization of n-GaAs electrodes was carried out in room-temperature molten-salt electrolytes by using the aluminum chloride–butylpyridinium chloride ($AlCl_3$–BPC) system as a representative example. The working potential limits for the above electrodes in the melts, containing varying ratios of $AlCl_3$ and BPC, were established by cyclic voltammetry. Flat-band potential (V_{fb}) measurements on n-GaAs in the same melts enabled location of the semiconductor band edge positions relative to the melt stability windows. In electrolytes containing $AlCl_3$ and BPC in the 1:1 molar ratio, the available range of potential was wide enough to probe the entire band-gap region. On the other hand, the potentials corresponding to the conduction band edges of n-GaAs were beyond the cathodic stability limit of both the 2:1 and 0.75:1 $AlCl_3$–BPC compositions. The electrode dissolution behavior of illuminated n-GaAs electrodes was investigated by cyclic voltammetry in melts of varying composition containing no intentionally added electroactive species. The onset of photoanodic corrosion currents was significantly positive of the values observed in aqueous electrolytes. The redox behavior of ferrocene–ferricenium ion couple ($Fe(Cp)_2/Fe(Cp)_2^+$) was studied by cyclic voltammetry on vitreous carbon electrodes in the 2:1, 0.75:1, and 1:1 $AlCl_3$–BPC electrolytes. This couple was electrochemically reversible in the above melts. Photogenerated holes on n-GaAs electrodes were competitively captured by the electrochemically active ferrocene species in the 1:1 $AlCl_3$–BPC electrolyte. This redox reaction occurred quite efficiently at the expense of the parasitic electrode dissolution process as judged by the constancy of photocurrents in a n-GaAs |1:1 $AlCl_3$–BPC||$Fe(Cp)_2/Fe(Cp)_2^+$|C PEC cell under short-circuit conditions for periods up to ~1 month. The underpotentials developed for the photoanodic process on n-GaAs relative to the reversible (dark) thermodynamic values on vitreous carbon were direct evidence for the sustained conversion of light energy to electrical energy. Rectifying behavior was observed on n-GaAs electrodes, with the reduction waves corresponding to the dark reduction of ferricenium chloride. The occurrence of this process at potentials positive of V_{fb} indicated the mediation of surface states in the electron-transfer process. Nonoptimized n-GaAs|1:1|$AlCl_3$–BPC||$Fe(Cp)_2/Fe(Cp)_2^+$|C PEC cells typically showed open-circuit potentials of 680 mV, fill factors around 0.49, and a net optical-to-electrical conversion efficiency of ~1% under illumination with a tungsten lamp at 40 mW/cm^2.

Introduction

Considerable attention has been focused in recent years on photoelectrochemical (PEC) conversion of light to electrical and chemical forms of energy.[1] The key element of PEC cells is the semiconductor photoelectrode. A perennial problem in the efficient operation of PEC devices has been the deleterious corrosion reactions undergone by the semiconducting electrodes, particularly in PEC cells employing aqueous electrolytes. Various approaches have been adopted to tackle this problem, and the parasitic reactions have been supressed to varying degrees of success (for a review of the literature on this topic, see ref 1h). The majority of these studies involve aqueous electrolytes which have at least three major disadvantages when compared with nonaqueous electrolytes: (a) a limited potential range (1.23 V) to work with, (b) the unfavorable shift in anodic decomposition potentials toward more negative values, and (c) fewer reversible one-electron redox couples that can be used without kinetic complication.

Therefore, a more profitable approach hinges on the use of nonaqueous electrolytes in PEC cells in place of aqueous electrolytes.[2-5] The feasibility of converting sunlight to electricity in PEC cells employing nonaqueous solvents has been demonstrated for at least two electrolyte systems, i.e., acetonitrile[2] and ethanol[3] although the reported conversion efficiencies are poor. A recent paper also reports on the photogeneration of solvated

*Address correspondence as follows: K.R., Department of Electrical Engineering; R.J., Department of Chemistry.

(1) (a) M. D. Archer, *J. Appl. Electrochem.*, **5**, 17 (1975); (b) J. Manassen, D. Cahen, G. Hodes, and A. Sofer, *Nature (London)*, **263**, 97 (1976); (c) H. Gerischer in "Semiconductor Liquid-Junction Solar Cells", A. Heller, Ed., The Electrochemical Society, Princeton, NJ, 1977, p 1 (see also references cited therein); (d) M. S. Wrighton, *Technol. Rev.*, **31**, May, 1977; (e) A. J. Nozik, *Annu. Rev. Phys. Chem.*, **29**, 89 (1978); (f) W. A. Gerrard and L. M. Rouse, *J. Vac. Sci. Technol.*, **15**, 1155 (1978); (g) L. A. Harris and R. H. Wilson, *Annu. Rev. Mater. Sci.*, **8**, 99 (1978); (h) K. Rajeshwar, P. Singh, and J. DuBow, *Electrochim. Acta*, **23**, 1117 (1978); (i) H. P. Maruska and A. K. Ghosh, *Sol. Energy*, **20**, 443 (1978); (j) M. Tomkiewicz and H. Fay, *Appl. Phys.*, **18** (1978).

(2) (a) S. N. Frank and A. J. Bard, *J. Am. Chem. Soc.*, **97**, 7427 (1975); (b) D. Laser and A. J. Bard, *J. Phys. Chem.*, **80**, 459 (1976); (c) P. A. Kohl and A. J. Bard, *J. Am. Chem. Soc.*, **99**, 7531 (1977); (d) P. A. Kohl and A. J. Bard, *J. Electrochem. Soc.*, **126**, 59 (1979); (e) *ibid.*, **126**, 598 (1979).

(3) K. D. Legg, A. B. Ellis, J. M. Bolts, and M. S. Wrighton, *Proc. Natl. Acad. Sci. U.S.A.*, **74**, 4116 (1977).

(4) R. E. Malpas, K. Itaya, and A. J. Bard, *J. Am. Chem. Soc.*, **101**, 2535 (1979).

(5) (a) M. Miyake, H. Yoneyama, and H. Tamura, *Electrochim. Acta*, **22**, 319 (1977); (b) K. Nakatani and H. Tsubomura, *Bull. Chem. Soc. Jpn.*, **50**, 783 (1977); (c) K. Nakatani, S. Matsudaira, and H. Tsubomura, *J. Electrochem. Soc.*, **125**, 406 (1978); (d) H. Tsubomura, M. Matsumura, K. Nakatani, K. Yamamoto, and K. Maeda, *Sol. Energy*, **21**, 93 (1978).

0002-7863/80/1502-4676$01.00/0

electrons on p-GaAs electrodes in ammonia.[4] One major disadvantage of the above solvents is their low electrical conductivity relative to aqueous media. In an attempt to surmount this difficulty, we have investigated the feasibility of using aprotic room-temperature molten salts in PEC cells. A variety of such salts have been described in the recent literature.[6] These electrolytes, in general, have good electrical conductivity in addition to the aforementioned positive features of nonaqueous solvents relative to aqueous electrolytes. In this paper, the above ideas are illustrated for n-GaAs electrodes in a well-characterized room-temperature molten-salt system consisting of mixtures of $AlCl_3$ and *n*-butylpyridinium chloride (BPC) in various molar ratios. We present detailed photoelectrochemical studies which show that in these electrolytes, photoanodic dissolution of n-GaAs can be effectively suppressed by the competitive photooxidation of the ferrocene/ferricenium redox couple. Evidence for sustained conversion of light energy to electrical energy is presented for illuminated n-GaAs electrodes in the 1:1 $AlCl_3$–BPC electrolyte. These results point toward a new avenue that could be explored profitably in the area of energy conversion utilizing PEC cells.

Experimental Section

Single crystals of tin doped n-GaAs were obtained from commerical sources. These crystals had reported resistivities in the range of 1×10^{-3} to 1×10^{-5} Ω cm. The crystals were chemomechanically polished with a ~2% solution of bromine in methanol after degreasing with xylene. Ohmic contacts were provided by thermal evaporation of Ge–Au alloy on the back surface and subsequent annealing in forming gas at 400 °C. A Teflon-covered copper wire was attached to the back contact by using silver epoxy. The entire back surface and edges of the electrodes were then covered with nonconducting epoxy resin. The ⟨111⟩ crystallographic face of the crystal was exposed to the electrolyte in all cases. The exposed electrode area, uncorrected for surface roughness, was ~4 mm^2. All electrodes were etched for 15 s in 3:1:1 H_2SO_4–30% H_2O_2–H_2O and then given a 30-s etch in 6M HCl. The electrodes were rinsed with deionized water, washed with ethyl alcohol, dried under vacuum, and then stored under an argon atmosphere in a Vacuum Atmospheres drybox.

The $AlCl_3$–BPC electrolytes were prepared by simple mixing of $AlCl_3$ and BPC in desired molar ratios. AnalaR grade $AlCl_3$ was further purified by sublimation in a sealed tube. BPC was prepared from *n*-butyl chloride and pyridine (1:1 molar quantities) by known procedures.[6e] All subsequent manipulations with these chemicals and electrolyte preparation were carried out in the drybox under argon atmosphere. Preparation of the 2:1 and 0.75:1 $AlCl_3$–BPC electrolytes followed a procedure described elsewhere.[7] The 1:1 $AlCl_3$–PBC electrolyte was prepared by simple mixing of the two components, and its composition was adjusted to the desired value by addition of $AlCl_3$/BPc by using a potentiometric titration procedure.[7] The 1:1 electrolyte composition was adjusted to be slightly on the acidic side to obtain a wider stability range (vide infra). Experiments with this electrolyte had to be carried out at a temperature slightly above ambient (~35 °C) in view of its higher melting point (31 ± 1 °C) relative to the 2:1 and 0.75:1 compositions which are liquid at room temperature.

Ferrocene obtained from commercial sources was purified by extraction with petroleum ether and subsequent recrystallization. Ferricenium chloride ($Fe(Cp)_2Cl$) was prepared by using standard procedures.[8] The ferrocene and ferricenium chloride concentrations used in the electrolyte were 58 and 6 mM, respectively.

A Pyrex cell of conventional design was employed for the electrochemical measurements. Standard three electrode geometry was employed for all potentiostatic measurements. The photoanode was positioned as close to the cell wall as possible to minimize light absorption by the electrolyte. The quasi-reference electrode was an Al wire immersed in the 2:1 electrolyte and separated from the working electrode compartment by a fine-porosity glass frit. All potentials quoted in this study are referred to this quasi-reference electrode (the potential of an Al wire in the 2:1 melt would lie about 0.12 V anodic of SCE on an absolute potential scale). A vitreous carbon plate (1.5 × 15 × 30 mm, Atomergic Chemetals Corp., N.Y.) was used as the counterelectrode for the electrochemical measurements. A 3-mm-diameter vitreous carbon rod sealed in a glass tube was used as the working electrode for cyclic voltammetry.

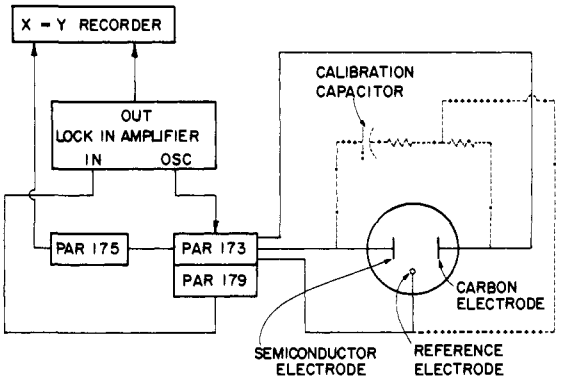

Figure 1. Schematics of the experimental setup for measuring the semiconductor capacitance as a function of applied bias. (Dotted lines represent the part of the circuit that replaces the cell in the calibration mode.)

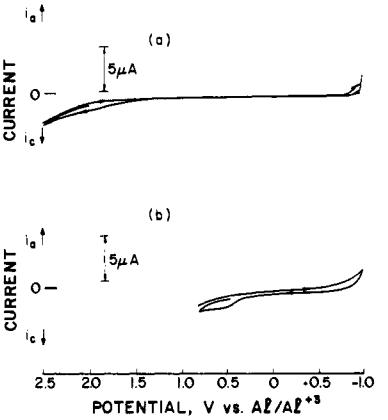

Figure 2. Background current on (a) n-GaAs and (b) vitreous carbon electrodes in the 1:1 $AlCl_3$–BPC molten-salt electrolyte. Scan rate: 20 mV/s.

Cyclic voltammetry was carried out on a Princeton Applied Research (PAR) Model 175 universal programmer, PAR 173 potentiostat/galvanostat, PAR 179 coulometer, and a Houston Instruments Model RE-0074 X-Y recorder. The working electrode was potentiostated against the quasi-reference electrode. Positive feedback compensation was employed to overcome resistive effects arising from electrode bulk and solution resistance.

Capacitance measurements were carried out in the frequency range 1–10 kHz by using a lock-in technique. A ~10 mV (peak to peak) sine wave signal was superimposed on a dc ramp. A PAR 175 universal programmer was used in conjunction with a 173 potentiostat/galvanostat combination to provide the dc ramp. The current flowing in the cell was detected by using a PAR 179 digital coulometer. An Ithaco Dynatrac 3 lock-in amplifier was used to detect the signal. The capacitance–voltage plot was recorded on a Houston RE-0074 X-Y plotter. A schematic of the experimental setup is shown in Figure 1. A scan rate of 5 mV/s was employed, and all experiments were performed in the dark.

A 150-W tungsten lamp was used to illuminate the semiconducting electrodes. The intensity of the light source was calibrated by using a neutral density filter and an Ealing Corp. Model LIMS 920 radiometer/photometer. The light intensities were not corrected for reflection and absorption losses in the cell and electrolyte.

A PAR 174 polarographic analyzer was used with a Houston Model RE-0074 X-Y recorder to obtain pulse polarograms where the photoanode was pulsed against the reference electrode. A scan rate of 2 mV/s and a pulse of 5 mV (peak to peak) were employed. Another set of photocurrent vs. potential data were obtained by using a Hewlett-Packard Model 721A power supply in series with the photoanode and the coun-

(6) (a) F. H. Hurley and T. P. Wier, Jr., *J. Electrochem. Soc.*, **98**, 207 (1951); (b) H. L. Chum, V. R. Koch, L. L. Miller, and R. A. Osteryoung, *J. Am. Chem. Soc.*, **97**, 3624 (1975); (c) V. R. Koch, L. L. Miller, and R. A. Osteryoung, *J. Am. Chem. Soc.*, **98**, 5227 (1976); (d) H. L. Chum, D. Koran, and R. A. Osteryoung, *J. Organomet. Chem.*, **140**, 349 (1977); (e) R. J. Gale, B. Gilbert, and R. A. Osteryoung, *Inorg. Chem.*, **17**, 2728 (1978); (f) C. L. Hussey, L. A. King, and R. A. Carpio, *J. Electrochem. Soc.*, **126**, 1029 (1979); (g) C. L. Hussey and L. A. King, *ibid.*, in press; (h) J. Robinson and R. A. Osteryoung, *J. Am. Chem. Soc.*, **101**, 323 (1979); (i) R. A. Carpio, L. A. King, R. E. Lindstrom, J. C. Nardi, and C. L. Hussey, *J. Electrochem. Soc.*, **126**, 1644 (1979); (j) J. Robinson, R. C. Bugle, H. L. Chum, D. Koran, and R. A. Osteryoung, *J. Am. Chem. Soc.*, **101**, 3776 (1979).

(7) R. J. Gale and R. A. Osteryoung, *Inorg. Chem.*, **18**, 1603 (1979).

(8) D. N. Hendrickson, Y. S. Sohn, and H. B. Gray, *Inorg. Chem.*, **10**, 1559 (1971).

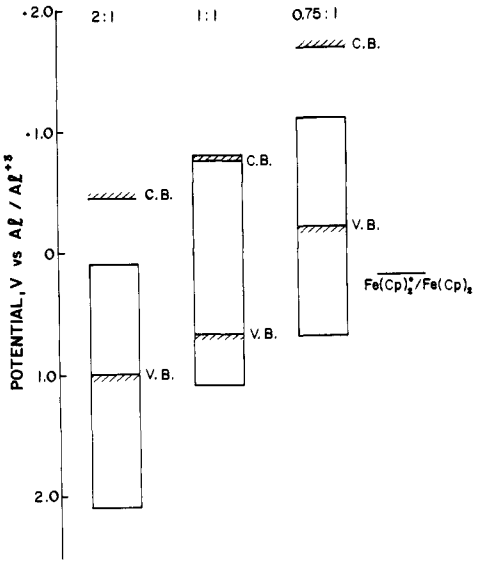

Figure 3. Positions of n-GaAs band edges and stability windows for the 2:1, 1:1, and 0.75:1 $AlCl_3$–BPC molten-salt electrolytes.

terelectrode. The current was measured as the potential drop across a 1 kΩ resistor in series in the external circuit.

Results

The range of potentials that are available with $AlCl_3$–BPC molten salts is critically dependent on the molar ratios of $AlCl_3$ and BPC.[6] A typical cyclic voltammogram obtained on a carbon electrode in the 1:1 electrolyte is shown in Figure 2b. The onset of anodic and cathodic currents at the potential limits of the cyclic voltammetry scans corresponds to decomposition of the electrolyte. The stability range determined from similar scans for the 2:1 and 0.75:1 compositions is shown in Figure 3, together with the potential limits for the 1:1 electrolyte. Also shown in Figure 3 are the conduction and valence band edges for n-GaAs in the three electrolytes. These were determined from flat-band potential (V_{fb}) measurements described below. It is pertinent to note that the potentials corresponding to the conduction band edges are beyond the range of accessibility in both the 2:1 and 0.75:1 electrolytes. Most of the studies described in the present paper, therefore, refer to the 1:1 composition in which the available range of potentials is wide enough to probe the entire band gap region. The stability range for all three compositions (~2.0 V) is greater than the 1.23 V available with aqueous electrolytes. This is a typical advantage in the use of aprotic solvents in PEC cells (see above and also ref 2 and 3).

Figure 2a is a cyclic voltammogram obtained on a n-GaAs electrode in the dark in the 1:1 $AlCl_3$–BPC molten salt electrolyte containing no deliberately added electroactive species. The electrolyte is seen to be stable over a wider potential range on n-GaAs than on the carbon electrodes. For example, the anodic current onset on n-GaAs lies 1.0 V anodic of the potential on vitreous carbon. Similarly, the cathodic working limit lies about 0.1 V cathodic of the potential on vitreous carbon electrodes. Similar behavior was observed for the 2:1 and 0.75:1 compositions. The enhanced electrolyte stability on n-GaAs in the dark relative to vitreous carbon can be ascribed to the reduced availability of minority carriers (holes in this case) for the electrolyte dissolution reaction in the dark. The much larger potential shift that is observed in the anodic range relative to the cathodic limit is also consistent with the behavior to be expected for a n-type semiconducting electrode.

Figure 4 shows the cyclic voltammograms obtained on illuminated n-GaAs electrodes in the 1:1 (Figure 4a) and 2:1 (Figure 4b) $AlCl_3$–BPC molten-salt compositions. The electrolytes contained no intentionally added electroactive species. Appreciable anodic currents are observed to flow at potentials positive of ~0.4 V in both cases. These currents typically show saturation effects in both quiet and stirred solutions, indicating that they are not

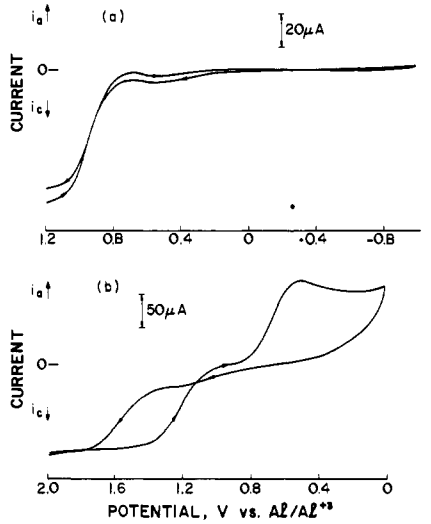

Figure 4. Cyclic voltammograms on illuminated n-GaAs in (a) 1:1 electrolyte (scan rate: 2 mV/s) and (b) 2:1 electrolyte (scan rate: 100 mV/s). The electrolyte in both cases contained no deliberately added redox species.

Table I. Cyclic Voltammetry Data for Vitreous Carbon Electrodes in 1:1 $AlCl_3$–BPC Molten-Salt Electrolyte Containing 13.6 mM Ferrocene

scan rate, mV/s	V_p^c, V	V_p^a, V	$V_p^a - V_p^c$, V	i_p^a/i_p^c	$i_p^c/\nu^{1/2}$, μA s$^{1/2}$ mV$^{-1/2}$
5	0.205	0.27	0.065	1.36	3.63
10	0.205	0.27	0.065	1.27	3.72
20	0.205	0.27	0.065	1.20	3.86
50	0.205	0.27	0.065	1.21	3.96
100	0.205	0.27	0.065	1.21	4.00
200	0.21	0.27	0.060	1.20	4.1

diffusion controlled. On the other hand, changes in the light intensity affect the limiting value of the photoanodic current as expected for a process which is controlled by the availability of photogenerated minority carriers (holes) at the electrode/electrolyte interface. These currents are attributed to the photodissolution of n-GaAs in the molten-salt electrolytes (vide infra). The cathodic reaction waves on the reverse scan in Figure 4b presumably arise from the reduction of electrode decomposition products by the electrolyte. No attempt was made to further characterize these parasitic reactions. The photoanodic currents also showed a pronounced time dependence, the currents dropping to low levels (<0.1 mA/cm^2) after a few hours of illumination. These current-blocking effects probably arise from the formation of insulating layers (e.g., corrosion products) on the electrodes after prolonged illumination in the PEC cell. Surface pitting of the electrode was also seen in a few instances. Similar effects on the photodissolution of n-GaAs electrodes in contact with aqueous electrolytes have been noted and discussed by previous authors.[2] It is also pertinent to note the large positive shift in the onset potentials for photodissolution of n-GaAs electrodes in $AlCl_3$–BPC electrolytes relative to the values observed in aqueous electrolytes (–0.58 V vs. SCE). A similar effect has been observed for n-GaAs in acetonitrile.[2d] Such anodic potential shifts for electrode dissolution are quite typical of nonaqueous solvents and represent an important advantage in the use of these electrolytes vis-à-vis aqueous electrolytes in PEC cells.

Cyclic voltammetry was carried out on carbon electrodes with a view to establish the redox behavior of the ferrocene/ferricenium ion couple in the $AlCl_3$–BPC melts of varying composition. Relevant data are presented in Table I for the 1:1 electrolyte. The separation between the anodic and cathodic peaks is very close to the theoretically predicted value of 59 mV, for a one-electron reversible redox process at the scan rates employed. The peak ratio i_p^a/i_p^c (estimated by the semiempirical procedure described in ref 9) is close to unity (Table I), indicating that the couple is

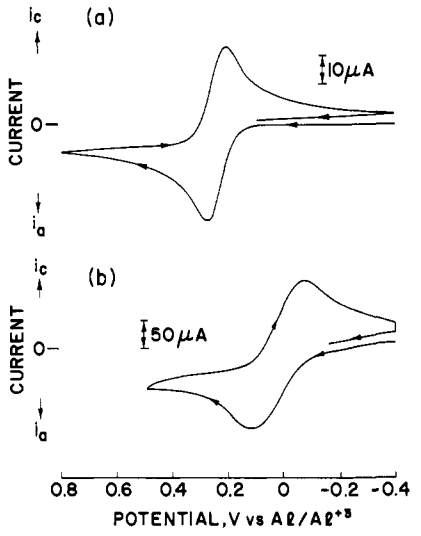

Figure 5. Comparison of cyclic voltammograms on (a) vitreous carbon and (b) illuminated n-GaAs. The electrolyte was 1:1 $AlCl_3$–BPC containing ferrocene. Light intensity in (b) was ~100 mW/cm^2. Scan rate: 100 mV/s. Redox concentration in (a) was 13.6 mM and in (b) 58 mM.

not complicated by homogeneous kinetic process in the range of scan rates employed. Essentially similar behavior has been reported by previous authors[6h] for the ferrocene/ferricenium couple in aluminum chloride–ethylpyridinium bromide.

Figure 5 compares the cyclic voltammograms on vitreous carbon (Figure 5a) and on illuminated n-GaAs (Figure 5b) in the 1:1 electrolyte. The electrolyte contained 58 mM ferrocene. Note that the oxidation wave on the GaAs electrode at a given scan rate appears at potentials 0.10–0.20 V cathodic of the corresponding value on vitreous carbon. Underpotentials for photoanodic currents in the range 150–250 mV were routinely observed for the various n-GaAs electrodes in the present study. This result furnishes direct evidence for the conversion of light to electrical energy on n-GaAs electrodes in the 1:1 $AlCl_3$–BPC electrolyte; i.e, electron transfer on the illuminated semiconductor electrode is accomplished with less applied electrical energy relative to the reversible carbon electrode in the dark. No waves are found for positive-going scans on n-GaAs in the dark—a behavior which is consistent with the rectifying nature of the n-GaAs/electrolyte interface. Reduction waves are seen at potentials positive of V_{fb} in the presence of ferricenium chloride in the 1:1 electrolyte. Table II summarizes the variation of the peak positions, V_p^a and V_p^c with scan rate with and without illumination for n-GaAs in the 1:1 electrolyte. The cathodic potential shift at faster scan rates is consistent with an inherently sluggish electron-transfer process in the dark.

Figure 6a shows current–voltage behavior of n-GaAs electrodes in the potentiostatic mode as a function of light intensity. The electrolyte in this case was 1:1 $AlCl_3$–BPC containing 58 mM ferrocene and 6mM ferricenium chloride. The dependence of the photocurrent saturation level on light intensity is characteristic of a process controlled by the availability of photogenerated minority carriers at the electrode/electrolyte interface (see above). The onset potential for photoanodic current flow is also seen to be a rather weak function of light intensity over the range of levels investigated in the present study. Figure 6b illustrates the current–voltage characteristics of a regenerative n-GaAs|1:1 $AlCl_3$–BPC||$Fe(Cp)_2^+/Fe(Cp)_2$|C cell, where $Fe(Cp)_2^+/Fe(Cp)_2$ represents the ferricenium/ferrocene redox couple. The current–voltage curves are shown for three light intensities. The output power typically peaks at 430 mV and the fill factors approach 0.49 for these cells. The optical to electrical conversion efficiency at the maximum power point is calculated to be ~1% at 40 mW/cm^2.

(9) R. S. Nicholson, *Anal. Chem.*, **38**, 1406 (1966).

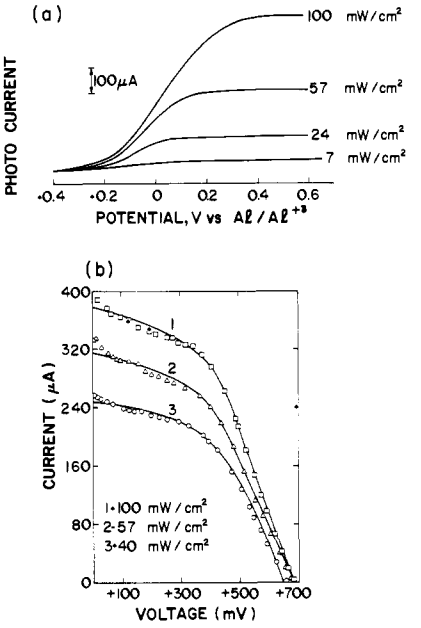

Figure 6. Current–voltage characteristics of n-GaAs in 1:1 $AlCl_3$–BPC electrolyte containing 58 mM ferrocene and 6 mM ferricenium chloride at different light intensities. The carbon counterelectrode was 0.24 V vs. the reference electrode; curves (a) were obtained under potentiostated condition. Scan rate: 2 mV/s.

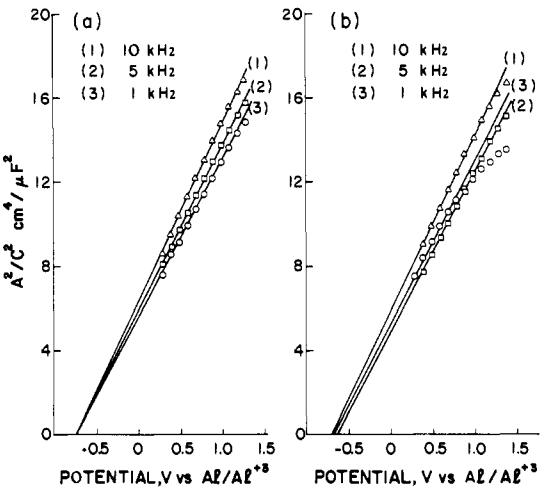

Figure 7. Mott–Schottky plots for n-GaAs in the dark in (a) 1:1 $AlCl_3$–BPC electrolyte and (b) 1:1 $AlCl_3$–BPC electrolyte containing 13.6 mM ferrocene.

Long-term irradiation of n-GaAs photoelectrodes was carried out in the 1:1 electrolyte with a view to test their stability. These tests were typically performed on cells under short-circuit conditions. Photocurrents were constant within the limits of experimental error for periods up to one month.

Mott–Schottky plots[10] constructed from space-charge capacitance measurements permitted determination of V_{fb} for n-GaAs electrodes in the various $AlCl_3$–BPC electrolyte systems. Illustrative results are shown for the 1:1 electrolyte in Figure 7a. A set of converging straight lines yield a common intercept on the potential axis. A V_{fb} value of −0.75 ± 0.02 V is deduced from such measurements in the 1:1 electrolyte. Donor densities, N_D,

(10) (a) E. C. Dutoit, R. L. Van Meirhaeghe, F. Cardon, and W. P. Gomes, *Ber. Bunsenges. Phys. Chem.*, **79**, 1206 (1975); (b) R. DeGryse, W. P. Gomes, F. Cardon, and J. Vennik, *J. Electrochem. Soc.*, **122**, 711 (1975); (c) E. C. Dutoit, F. Cardon, and W. P. Gomes, *Ber. Bunsenges. Phys. Chem.*, **80**, 475 (1976); (d) W. H. Laflere, R. L. Van Meirhaeghe, F. Cardon, and W. P. Gomes, *Surf. Sci.*, **59**, 401 (1976); (e) M. J. Madou, F. Cardon, and W. P. Gomes, *J. Electrochem. Soc.*, **124**, 1623 (1977); (f) F. Cardon and W. P. Gomes, *J. Phys. D*, **11**, 163 (1978).

Table II. Cyclic Voltammetry Data on n-GaAs Electrodes in 1:1 $AlCl_3$–BPC Electrolyte Containing 58 mM Ferrocene and 6 mM Ferricenium Chloride

scan rate, mV/s	peak potentials: dark V_p^c, V	dark V_p^a, V	illuminated V_p^c, V	illuminated V_p^a, V
10	0.01	...	0.0	0.06
20	0.01	...	−0.03	0.07
50	−0.01	...	−0.06	0.09
100	−0.025	...	−0.08	0.12
200	−0.05	...	−0.11	0.17

calculated from the slopes of such plots are approximately 10^{19} cm^{-3}. Figure 7b shows Mott–Schottky plots for GaAs in the 1:1 electrolyte with added ferrocene. A V_{fb} of −0.70 ± 0.050 V is obtained from these data. The good correlation of this value with that obtained in the absence of ferrocene suggests negligible specific adsorption of ferrocene/ferricenium redox species on the electrode surface. This behavior also contrasts the situation observed with CdX (X = S, Se, Te) electrodes in polychalcogenide electrolytes where the flat-band potential depends smoothly on the X^{2-} concentration.[11] The V_{fb} values, however, do depend on the relative amounts of $AlCl_3$ and BPC in the molten-salt electrolytes as discussed below.

The positions of the conduction and valence band edges were determined in the usual manner[12] from the measured V_{fb} values in $AlCl_3$–BPC melts of different composition. Typical results are shown in Figure 3. For these determinations it was assumed that $E_{CB/e_0} = V_{fb}$, an assumption which is justified for the carrier densities found for n-GaAs samples used in this study. The conduction band edge is seen to shift to more negative potentials with increasing basicity of the electrolyte. A similar negative shift was recently reported for n-GaAs electrodes in liquid ammonia.[4] These potential shifts are characteristics of specific adsorption of electrolyte species on the electrode surface (see above). Work is in progress in these laboratories on the elucidation of the nature of electrolyte adsorption and chemical identification of adsorbed species giving rise to these effects.

Discussion

The results presented in this paper serve to illustrate the applicability of molten salts such as the $AlCl_3$–BPC system to photoelectrochemical systems in general. Regenerative PEC cells have been constructed with n-GaAs electrodes in these molten-salt electrolytes. The stable output generated by such cells is a direct indication that photogenerated holes are competitively captured in the redox process at the expense of the parasitic electrode dissolution reaction. One aspect of this study which merits further discussion is the effect of electrolyte composition on the photoelectrochemical behavior of n-GaAs electrodes. In contrast to the results obtained with the 1:1 $AlCl_3$–BPC electrolyte, both 2:1 and 0.75:1 compositions failed to yield stable photocurrents with the $Fe(Cp)_2^+/Fe(Cp)_2$ couple. Electrode dissolution also seemed to be quite facile in these electrolytes. Factors contributing to these electrolyte effects are to be sought in the relative positions of the semiconductor band edges with respect to the decomposition potential (E_D) and the redox level.[13] In this regard, the stabilizing effect of the $Fe(Cp)_2^+/Fe(Cp)_2$ couple is readily rationalized on the basis of energy-band diagrams such as the one illustrated in Figure 3. A comparison of the $Fe(Cp)_2^+/Fe(Cp)_2$ level with the valence band edges for the three electrolyte compositions shown

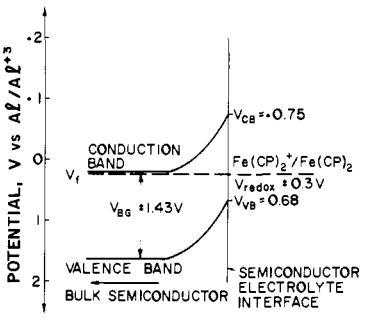

Figure 8. Interfacial energetics for n-GaAs in the 1:1 $AlCl_3$–BPC electrolyte containing $Fe(Cp)_2^+/Fe(Cp)_2$ redox couple.

in Figure 3 reveals that in the case of the 0.75:1 electrolyte this couple will be ineffective in capturing the photogenerated holes on n-GaAs. Similarly the absence of a stable photoeffect for the 2:1 electrolyte can be traced to the possible lack of significant overlap of the energy levels corresponding to the reduced redox species with the valence band edge of n-GaAs as required by the Gerischer model.[14] In line with the arguments above, one would predict the 1:1 electrolyte to be the most likely candidate for regenerative n-GaAs|$AlCl_3$–BPC|$Fe(Cp)_2^+/Fe(Cp)_2$|C cells. This prediction is indeed borne out by the experimental results described above. The results from cyclic voltammetry for this electrolyte also fit into this general pattern in a straightforward manner.

Although the Gerischer model[14] is adequate in explaining the overall photoelectrochemical behavior of n-GaAs in $AlCl_3$–BPC melts, a more careful inspection of the present experimental data reveals features which necessitate modification of the simple band model. It is pertinent to note in this regard that measurable rates of reduction were sustained for n-GaAs electrodes in the dark in the 1:1 electrolyte at potentials *well positive* of V_{fb}. A possible explanation for this hinges on the presence of surface states which mediate electron transfer in the intraband gap region. Such a mechanism has been proposed before for n-GaAs and other semiconducting electrodes in acetonitrile.[2d] The finding that in the absence of electroactive species photoanodic corrosion currents were not observed on n-GaAs electrodes in the 1:1 electrolyte until the potentials were well positive of +0.3 V indicates that these surface levels are quite effective in acting as recombination centers for the photogenerated holes. In the presence of a redox couple such as $Fe(Cp)_2^+/Fe(Cp)_2$ which would conceivably overlap with the trap levels, the rate of filling of these levels by electrons from the redox species could be enhanced under illumination, leading to effective capture of the photogenerated holes. In the dark, such a process is not favored because of the slow rate of emptying of the traps into the conduction band. The rate at which the trap levels are populated by the solution species, and thus the extent of overlap of the energy levels of the reduced form of the redox species with those levels,[14] may be the determining factor in the stabilization of the semiconductor.

Figure 8 depicts the electrostatic aspects of the interface for n-GaAs in the dark in the 1:1 electrolyte. The maximum output potential that is attainable with a cell utilizing the $Fe(Cp)_2^+/Fe(Cp)_2$ couple in the 1:1 electrolyte is $V_{redox} - V_{fb}$ or $E_{G/e_0} - \phi_n$ (where ϕ_n = difference between the Fermi potential and the conduction band edge), whichever is smaller.[15] From Figure 8, this value is seen to be ~1 V. The V_{OC} values that were routinely observed for *n*-GaAs|1:1 $AlCl_3$–BPC||$Fe(Cp)_2^+/Fe(Cp)_2$|C cells in the present study are 60–70% of the maximum output. No attempts were made in the present study to overcome the possible influence of surface states by appropriate surface treatment nor were efforts directed toward improving cell performance by optimization of cell geometry. The feasibility of energy conversion

(11) M. S. Wrighton, J. M. Bolts, A. B. Bocarsly, M. C. Palazzolto, and E. G. Walton, *J. Vac. Sci. Technol.*, **15**, 1429 (1978).
(12) W. P. Gomes and F. Cardon, *Z. Phys. Chem. (Wiesbaden)*, **86**, 330 (1973).
(13) (a) H. Gerischer, *J. Electroanal. Chem.*, **58**, 263 (1975); (b) H. Gerischer, *ibid.*, **82**, 133 (1977); (c) A. J. Bard and M. S. Wrighton, *J. Electrochem. Soc.*, **124**, 1706 (1977); (d) H. Gerischer, *J. Vac. Sci. Technol.*, **15**, 1422 (1978).
(14) H. Gerischer in "Physical Chemistry—An Advanced Treatise", Vol. 9A, H. Eyring, D. Henderson, and W. Jost, Eds., Academic Press, New York, p 170, Chapter 5.
(15) S. Kar, K. Rajeshwar, P. Singh, and J. DuBow, *Sol. Energy*, **23**, 129 (1979).

utilizing n-GaAs electrodes in $AlCl_3$–BPC molten salts and the good stability demonstrated by these electrodes in the 1:1 electrolyte are encouraging. The results described above also suggest that considerable scope exists in the use of molten salts as electrolytes in photoelectrochemical systems.

Acknowledgments. The authors express their appreciation to the Solar Energy Research Institute and the U.S. Department of Energy for financial support of this research program. Thanks are also due to R. J. Gale for stimulating discussions on molten-salt electrolytes.

The High-Spin ($^5T_2$) ⇌ Low-Spin ($^1A_1$) Transition in Solid Bis(1,10-phenanthroline-2-carbaldehyde phenylhydrazone)iron(II) Diperchlorate. Simultaneous Change of Molecular Spin State and Crystallographic Structure

E. König,*[1a] G. Ritter,[1b] W. Irler,[1b] and H. A. Goodwin[2]

Contribution from the Institut für Physikalische und Theoretische Chemie and Physikalisches Institut, Abt. II, University of Erlangen-Nürnberg, D-8520 Erlangen, West Germany, and the School of Chemistry, The University of New South Wales, Kensington, N.S.W. 2033, Australia.
Received October 22, 1979

Abstract: The six-coordinate iron(II) complex $[Fe(phy)_2](ClO_4)_2$ (phy = 1,10-phenanthroline-2-carbaldehyde phenylhydrazone) has been shown by variable-temperature ^{57}Fe Mössbauer effect, X-ray diffraction, and magnetic measurements to exhibit a high-spin ($S = 2$; $^5T_2$) ⇌ low-spin ($S = 0$; $^1A_1$) transition in the solid state. The ground states involved are characterized, at the transition temperature T_c, by $\Delta E_Q(^5T_2) = 0.91$ mm s^{-1}, $\delta^{IS}(^5T_2) = +0.93$ mm s^{-1} and $\Delta E_Q(^1A_1) = 1.61$ mm s^{-1}, $\delta^{IS}(^1A_1) = +0.28$ mm s^{-1}. For sample I of $[Fe(phy)_2](ClO_4)_2$, a pronounced hysteresis of $\Delta T_c = 8.1$ K has been observed, the transition being centered at $T_c\uparrow = 256.1$ K for rising and at $T_c\downarrow = 248.0$ K for lowering of temperature. The Debye–Waller factors at $T_c\uparrow$ ($f_{^5T_2} = 0.116$, $f_{^1A_1} = 0.198$) show a discontinuity of $\Delta f_{total} \approx 42\%$, the temperature function of both $f_{^5T_2}$ and $f_{^1A_1}$ being well reproduced within the high-temperature approximation of the Debye model ($\Theta_{^5T_2} = 127.3$ K, $\Theta_{^1A_1} = 146.8$ K, $M_{Fe} = 57$ au). The X-ray diffraction patterns for the $^5T_2$ and $^1A_1$ phases are characteristically different. The temperature dependence of the molecular fraction $n_{^5T_2}$, including details of the hysteresis curve, is the same whether determined from the Mössbauer data or the X-ray peak profiles. Thus a concomitant change in the electronic state of the molecules and crystallographic properties of the lattice occurs at T_c. The $^5T_2 \rightleftharpoons {}^1A_1$ transition is thermodynamically first order. The observed equal areas of scanning curves are indicative, within the Everett model, of the formation of independent domains by both $^5T_2$ and $^1A_1$ molecules. From the line widths of X-ray diffraction patterns, the magnitude of the domains follows as ≥5000 Å. In a second sample, sample II of $[Fe(phy)_2](ClO_4)_2$, the first-order character of the $^5T_2 \rightleftharpoons {}^1A_1$ transition is diminished presumably due to impurities and/or defects in the solid. After recrystallization, sample II gives results similar to those of sample I.

Introduction

Temperature- or pressure-induced transitions between two states of differing spin multiplicity have been observed in certain complexes of d^5, d^6, d^7, and d^8 ions of the first-transition series.[3-5] The high-spin ($^5T_2$) ⇌ low-spin ($^1A_1$) transition which is characteristic for the (approximately octahedral) six-coordinated d^6 configuration has been also encountered in certain perovskites like $LaCoO_3$[6] and in mixed sulfides of the type $Fe_xTa_{1-x}S_2$.[7] Moreover, the variable spin state of iron proteins is believed to be of importance for the catalytic properties of these bioactive systems.[8] In solution, the spin interconversion process is dynamic in nature, and its mechanism seems to be reasonably well understood.[9,10] Thus rate constants for the process

$$\text{low spin} \underset{k_{-1}}{\overset{k_1}{\rightleftharpoons}} \text{high spin}$$

have been determined for a number of spin-interconversion systems and for iron(II) complexes; for example, the values obtained for k_1 and k_{-1} vary between 4×10^5 and 2×10^7 s^{-1}.[11]

The first example of a high-spin ($^5T_2$) ⇌ low-spin ($^1A_1$) transition was established for a solid complex,[12] and most subsequent studies have been concerned with systems in the solid state. Recent progress with spin transitions in the solid state has, however, been slow due to unpredictable lattice effects arising from variable degrees of solvation, different crystal forms of the same complex, or perhaps even the influence of slight differences in the

(1) (a) Institut für Physikalische und Theoretische Chemie, University of Erlangen-Nürnberg. (b) Physikalisches Institut, Abt. II, University of Erlangen-Nürnberg.
(2) School of Chemistry, University of New South Wales.
(3) R. L. Martin and A. H. White, *Transition Met. Chem.*, **4**, 113 (1968).
(4) E. König, *Ber. Bunsenges. Phys. Chem.*, **76**, 975 (1972).
(5) H. A. Goodwin, *Coord. Chem. Rev.*, **18**, 293 (1976).
(6) V. G. Bhide, D. S. Rajona, G. Rama Rao, and C. N. R. Rao, *Phys. Rev. B*, **6**, 1021 (1972).
(7) M. Eibschütz, M. E. Lines, and F. J. Di Saloo, *Phys. Rev. B*, **15**, 103 (1977).
(8) E. V. Dose, M. F. Tweedle, and L. J. Wilson, *J. Am. Chem. Soc.*, **99**, 3886 (1977).
(9) J. K. Beattie, R. A. Binstead, and R. J. West, *J. Am. Chem. Soc.*, **100**, 3044 (1978).
(10) R. A. Binstead, J. K. Beattie, E. V. Dose, M. F. Tweedle, and L. J. Wilson, *J. Am. Chem. Soc.*, **100**, 5609 (1978).
(11) E. V. Dose, M. A. Hoselton, N. Sutin, M. F. Tweedle, and L. J. Wilson, *J. Am. Chem. Soc.*, **100**, 1141 (1978).
(12) E. König and K. Madeja, *Inorg. Chem.*, **6**, 48 (1967).

0002-7863/80/1502-4681$01.00/0